Aggregation Properties of Amide Bearing Cleavable Gemini Surfactants by Small Angle Neutron Scattering and Conductivity Studies

Jiaul Hoque,[†] Pratik Kumar,[†] Vinod K. Aswal,[‡] and Jayanta Haldar*,[†]

[†]Bioorganic and Medicinal Chemistry Laboratory, New Chemistry Unit, Jawaharlal Nehru Centre for Advanced Scientific Research, Jakkur, Bengaluru 560064, India

[‡]Solid State Physics Division, Bhabha Atomic Research Centre, Mumbai 400085, India

S *Supporting Information*

ABSTRACT: The micellar aggregation of different amide bearing cleavable gemini surfactants with varying methylene spacer chain length (m = 2, 4, 6, 8, and 12) along with the corresponding monomeric surfactant in aqueous media has been investigated by conductometric and small angle neutron scattering (SANS) studies. The critical micellar concentration (CMC) values of gemini surfactants were found to be very low (CMC = 0.08−0.19 mM) and were 23−55 times lesser than the corresponding monomeric analogue (CMC = 4.4 mM). With increase in the spacer chain length, CMC was found to

Monomeric surfactant   Gemini surfactants

decrease whereas the degree of ionization was found to increase. SANS data have been analyzed by considering the screened Coulombic interactions between the micelles to compute the interparticle structure factor $S(Q)$. The extent of micellar growth and the variation of shapes of the micelles formed by these new surfactants in aqueous solution have been found to depend strongly on the spacer chain length. It was observed that the extent of micellar growth and variation of micellar shapes are more pronounced for surfactants with short spacer chain length ($m \leq 4$), whereas the surfactants with a long spacer chain length ($m \geq 6$) showed slight variation of these properties in aqueous solution. The effects of the variation of the concentration and temperature on the SANS spectra (and hence on the microstructure) of the gemini surfactant (m = 4) were also examined. With an increase in concentration the aggregation number (N) and size of the micelles (the ratio of semimajor axis (a) to semiminor axis ($b = c$)) increased whereas opposite phenomena was observed with an increase in temperature.
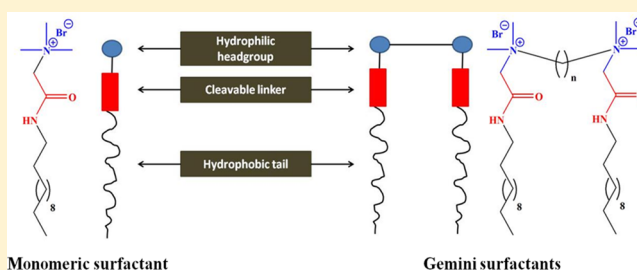
INTRODUCTION

Gemini surfactants, composed of two monomeric surfactant molecules chemically bonded together at or near their headgroups by a spacer, drew attention due to their superior properties over the conventional monomeric surfactants (composed of a polar headgroup and a hydrophobic chain).[1−14] Several reasons can be given for the present interest in gemini surfactants. First, their critical micellar concentration (CMC) is generally at least 1 or 2 orders of magnitude lower than that of the corresponding monomeric surfactants.[9] Second, they are 10−100 times more efficient at reducing the surface tension of water and the interfacial tension of the oil−water interface than the conventional surfactants.[10] Third, the aqueous solutions of some gemini surfactants with a short spacer can have extremely interesting rheological properties.[11,12] Additionally, the microstructure of some gemini surfactant solutions shows unusual but remarkable micellar shapes.[13,14] These constitute a few among the many advantages of gemini surfactants over monomeric surfactants.

Owing to such superior properties, gemini surfactants have been considered surfactants for the future. They have been used in various areas, such as skin and body care products,[15] food

industry,[16] phase transfer catalysts,[17] oil recovery,[18] gene delivery,[19,20] drug entrapment and release,[21] antimicrobial products,[22] etc. Recently they have also found their way in synthesizing various mesoporous and nanostructured materials.[23−27]

However, environmental concerns and aquatic toxicity limit the practical usage of the nondegradable surfactants.[28] In general, the conventional noncleavable gemini surfactants like dicationic ammonium compounds bearing long alkyl chains and a methylene spacer are toxic and irritating to skin and eyes.[29] Therefore, it is worthwhile to develop biodegradable and more eco-friendly surfactants and study their aggregation properties in aqueous solution in order to find their utility in household, biomedical and industrial applications.[30−32] The main approach to the design of these biodegradable (cleavable or soft) surfactants is the insertion of ester[33] or amide[34] bonds in the molecule, which limits their stability.[35,36]
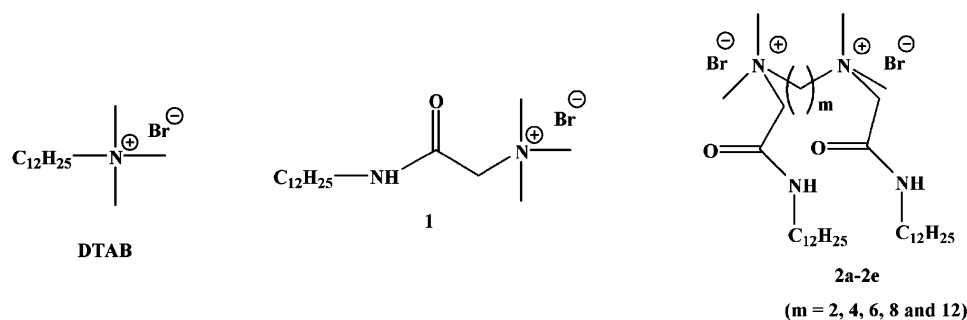
Figure 1. Structures of various cationic surfactants used in the study.
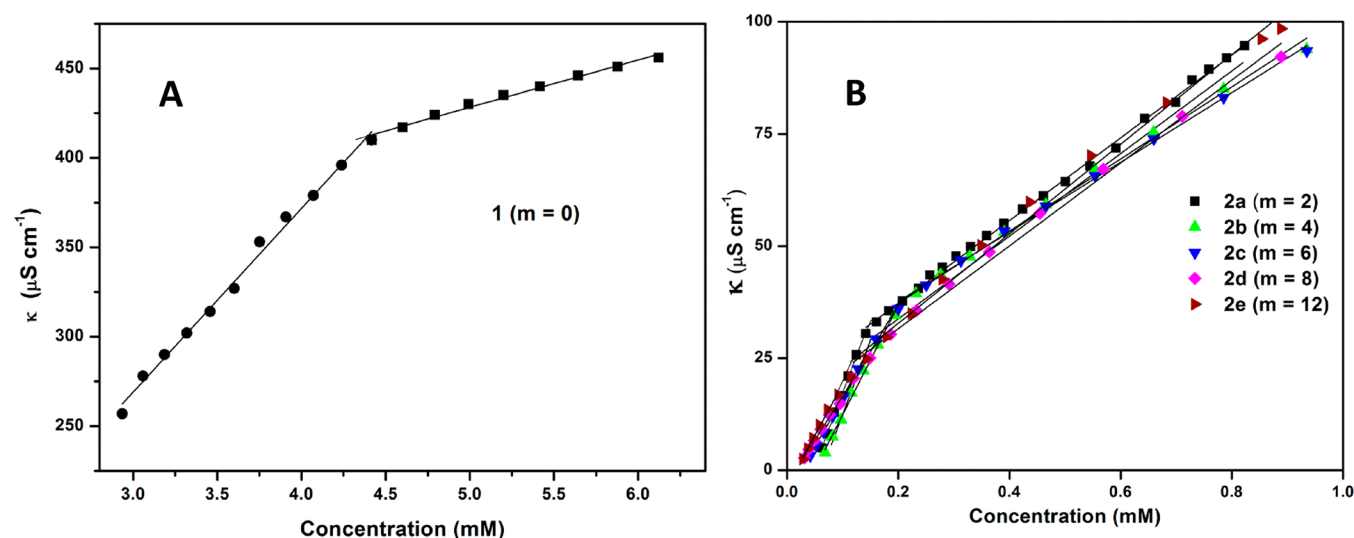

Figure 2. Plot of electrical conductivity (κ) vs surfactant concentrations: (A) for monomeric surfactant (**1**) and (B) for gemini surfactants (**2a−2e**).

Herein, we report a series of cationic gemini surfactants with different methylene spacers bearing cleavable amide linkages in between the polar headgroup and the hydrocarbon tail (Figure 1) and the study of their aggregation behavior by SANS and conductivity methods. SANS, being a noninvasive and reliable technique, has been used before extensively for the characterization of the micellar solutions of different surfactants,[37−46] including those of gemini surfactant.[47,48] In this study, we have investigated the role of the spacer chain length and the effect of the amide group in determining microstructure of these newly synthesized gemini surfactants in aqueous solution. The effect of variation in concentration and temperature on the neutron scattering cross sections was also examined. The critical micellar concentrations and the degrees of ionizations were determined by conductometic studies. The micellar aggregation properties of amide bearing gemini surfactants were compared with the corresponding monomeric surfactant (**1**).

■ EXPERIMENTAL SECTION

Materials. Synthesis of the amide bearing surfactants is given in the Supporting Information. Dodecylamine, bromoacetyl bromide, α,ω-dibromoalkanes, N,N,N′,N′-tetramethyl-1,2-diaminoethane, and dodecyltrimethylammonium bromide (DTAB) were purchased from Sigma-Aldirch Co. D_2O (99.5 at. % D), obtained from the Heavy Water Division of BARC, India, was used for the SANS studies. All of the reagents and solvents used in this study were of the analytical grade. Double distilled Millipore water was used for conductivity measurements. All of the surfactants were characterized by FT-IR,

^{1}HNMR, and high resolution mass spectrometry (HRMS) (Supporting Information).

Conductivity Measurements. The electrical conductivity method was employed to determine the critical micellar concentration (CMC) of the surfactants at 28 ± 0.3 °C using EUTECH CON 501 Cyberscan Conductivity Meter having cell constant 1.0. Millipore water (specific conductivity 0.055 μS cm^{-1} at 25 °C) was used to prepare the solutions for all of the surfactants. Concentrated solutions of individual surfactants of known concentrations were prepared. Solutions were then progressively diluted and the specific conductivity values were measured. The CMC values for each surfactant were determined as the cross point of the two straight lines by plotting the values of the specific electrical conductivity, κ against the surfactant concentration, C (Figure 2). The degree of ionization (α) of the micelles was calculated from the ratio of the slopes of the two straight lines above and below the CMC (Table 1). The variation of CMC and α values of micelles were established for surfactants with different spacer (Figure 3).

Small Angle Neutron Scattering (SANS) Measurements. *Data Collection.* Small angle neutron scattering (SANS) experiments were carried out with the aqueous solution (D_2O) of amide bearing monomeric **1** and gemini (**2a−2e**, m = 2, 4, 6, 8, and 12) surfactants. D_2O provides a very good contrast between the micelle and the solvent in a SANS experiment. Neutron-scattering measurements were performed on SANS instrument at the Dhruva Reactor, Trombay, India. The sample-to-detector distance was 1.8 m for all runs. This spectrometer makes use of a crystalline BeO filtered beam to

Table 1. CMC, Degree of Ionization (α), Scattering Length Density and Volume of Surfactant Monomer for Cationic Amide Bearing Surfactants[a]

surfactants	CMC (mM)	α	scattering length density ($\times 10^{10}$ cm^{-2})	volume of surfactant (Å^3)
1 ($m = 0$)	4.4	0.26	−0.016	543
2a ($m = 2$)	0.19	0.28	0.047	1231
2b ($m = 4$)	0.15	0.33	0.031	1288
2c ($m = 6$)	0.14	0.37	0.018	1344
2d ($m = 8$)	0.11	0.47	0.005	1400
2e ($m = 12$)	0.08	0.43	−0.017	1513

[a]CMC and α were determined by electrical conductivity method. Scattering length density for all the surfactants was calculated from SANS study. Volume of the surfactants was calculated by using Tanford's formula[42] and refs 49−52 and 57−59.

provide a mean wavelength λ of 0.52 nm and wavelength resolution ($\Delta\lambda/\lambda$) of about 15%. The angular distribution of the scattered neutrons is recorded using a one-dimensional position-sensitive detector (PSD). The accessible wave vector transfer, Q ($= 4\pi \sin \frac{1}{2}\theta/\lambda$, where θ is the scattering angle), range of this instrument is between 0.018 and 0.35 Å^{-1}. PSD allows a simultaneous recording of the data over the full Q range.

The solutions were held in a UV grade quartz sample holder (path length 0.2 cm) with tight-fitting Teflon stoppers, sealed with parafilm. SANS measurements for all the gemini surfactants were carried out with two different surfactant concentrations (C = 25 and 50 mM) at two different temperatures (30 and 60 °C). SANS experiments were also done for the monomeric surfactant **1** using 50 and 100 mM and for DTAB at 100 mM at 30 °C. The effect of concentration on the SANS distribution was studied for the gemini surfactant **2b** ($m = 4$) in the concentration range of 12.5−50 mM at 30 °C. Similarly, the effect of temperature was also investigated for the **2b** ($m = 4$) micellar system at 50 mM in the temperature range of 30−60 °C.

Data Treatment. Scattering intensities from the surfactant solutions were corrected for detector background and

sensitivity, empty cell scattering, and sample transmission. Solvent intensity was subtracted from that of the sample. The resulting corrected intensities were normalized to absolute cross section units and thus dΣ/dΩ vs Q was obtained. This absolute calibration has an estimated uncertainty of 10%. The experimental points are fitted using a nonlinear least-squares routine as described below. Comparisons between the experimental and the calculated cross sections are shown in Figures 4−8 and the fitted parameters are mentioned in Tables 2−6.
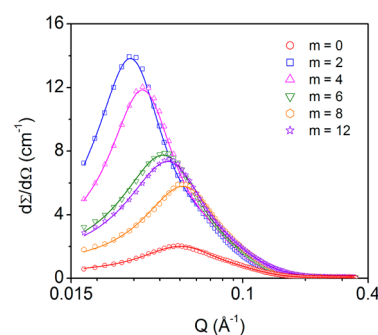

Figure 4. SANS distributions of the aqueous solution of gemini surfactants **2a**−**2e** ($m = 2−12$) and corresponding monomeric surfactant **1** ($m = 0$) at 50 mM concentration at 30 °C. The lines shown are theoretical fits and the solid marks are experimentally determined data points.

Analysis of SANS Data. *Calculation of the Scattering Intensity.* The coherent differential scattering cross section, dΣ/dΩ, derived by Hayter and Penfold[49−52] and Chen,[53,54] can be reduced for an assembly of monodispersed, uniform ellipsoidal micelles, as given by

$$d\Sigma/d\Omega = nV_m^2(\rho_m - \rho_s)^2 P(Q)S(Q) \qquad (1)$$

where n denotes the number density of the micelles, ρ_m and ρ_s are respectively the scattering length densities of the micelle and the solvent, and V_m is the volume of the micelle. $P(Q)$ is the single (orientationally averaged) intraparticle structure
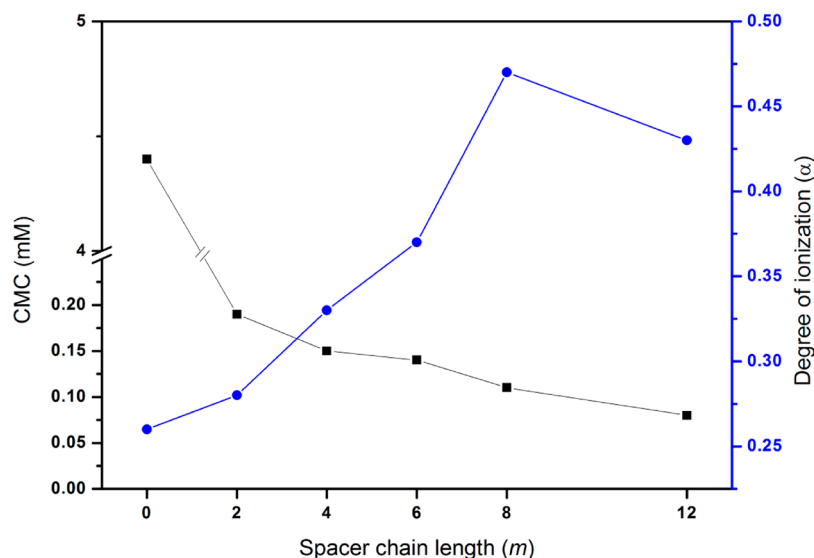

Figure 3. Variations of the CMC and degree of ionization (α) of the amide bearing surfactants with the spacer chain length (for monomeric surfactant $m = 0$ and gemini surfactants $m = 2, 4, 6, 8,$ and 12) at 28 °C.

Table 2. Effect of Spacer Length (m) in Micellar Systems of Amide Bearing Cationic Surfactants on Q Value[a]

micellar system	aggregation no., N	fractional charge, α	semimajor axis, a (Å)	semiminor axis, $b = c$ (Å)	a/b
DTAB	70	0.24	27.2	16.7	1.22
1 ($m = 0$)[b]	107	0.19	39.9	18.7	2.14
1 ($m = 0$)[c]	96	0.23	34.5	18.9	1.83
2a ($m = 2$)	585	0.09	396.5	20.2	19.63
2b ($m = 4$)	320	0.14	253.8	19.7	12.88
2c ($m = 6$)	125	0.18	105.9	20.4	5.19
2d ($m = 8$)	65	0.23	62.3	18.7	3.33
2e ($m = 12$)	104	0.19	107.1	18.7	5.72

[a]All of the SANS spectra were recorded at 30 °C using 100 mM for DTAB. [b]50 mM. [c]100 mM for monomeric surfactant 1 and 50 mM for all the dimeric surfactants (2a−2e).

factor, and $S(Q)$ is the interparticle structure factor. The aggregation number N for the micelle is related to the micellar volume V_m by the relation $N = V_m/\nu$, where ν is the volume of the individual surfactant molecule (Table 1). The volume of the surfactants 1 ($m = 0$) and 2a−2e ($m = 2, 4, 6, 8$ and 12) was found to be 543, 1231, 1288, 1344, 1400, and 1513 Å³, respectively. Volume of the monomeric surfactant 1 was calculated as follows:

$$V_{total} = (V_{hc} + V_{hg} + V_{linker})$$

where V_{hc} is the volume of the $-C_{11}H_{23}$ hydrocarbon tail (calculated by Tanford's formula[38] and found to be 323 Å³), V_{hg}, volume of the headgroup is 102 Å³ (as taken from the literature[50−52]), and V_{linker}, volume of linker ($-CH_2NHCOCH_2-$) part is 118 Å³ ($V_{linker} = M/dN_A$, where $M = 71$ is the molecular weight of the linker, $d = 1$ g cm⁻³ is the density, and N_A is the Avogadro's Number).[55] The volume of the gemini surfactants 2a−2e were calculated as follows:

$$V_{total} = [2\{V_{hc} + (2V_{CH_3}) + V_N + V_{linker}\} + mV_{CH_2}]$$

where V_{hc} is the volume of the $-C_{11}H_{23}$ hydrocarbon chain as calculated before, V_{linker}, volume of linker ($-CH_2NHCOCH_2-$) part is 118 Å³, $V_{CH_3} = 42.6$ Å³, the volume of the methyl groups attached to quaternized nitrogen atom has been taken from the literature,[47] $V_N = 30.5$ Å³, the volume of quaternized nitrogen atom, and $V_{CH_2} = 28.2$ Å³, the volume of the methylene groups (spacer, m).

The eq 1 can also be rewritten as follows

$$dS/dW = cN(b_m - n r_s)^2 P(Q)S(Q) \tag{2}$$

where c (=nN) is the surfactant concentration and b_m (=$\rho_m \nu$) is the total coherent scattering amplitude of the surfactant molecule.

The form factor $P(Q)$ for an ellipsoidal particle is given by

$$P(Q) = \int [F(Q\mu)]^2 \, d\mu \tag{3}$$

where $F(Q)$ is calculated as

$$F(Q, \mu) = 3(\sin w - w \cos w)/w^3 \tag{4}$$

$$w = Q[a^2\mu^2 + b^2(1 - \mu^2)]^{1/2} \tag{5}$$

where a and b are respectively the semimajor and semiminor axes of the ellipsoid of revolution. μ is the cosine of the angle between Q and a.

Structure Factor for Interacting Micelles. The interparticle structure factor $S(Q)$ has been found to depend on the spatial distribution of micelles. Unlike the calculation of $P(Q)$, it is

quite complicated to calculate $S(Q)$ for any other shape than spherical. This is because of $S(Q)$ depends on the shape as well as on the orientation of the particles and there are no analytical expressions available to calculate it for asymmetric particles. To simplify this, prolate ellipsoidal micelles are usually assumed to be equivalent spherical. In the following analysis, we calculate $S(Q)$ using rescaled mean spherical approximation as developed by Hansen and Hayter.[51] The ellipsoidal micelle is approximated by an equivalent sphere of radius $R = (ab^2)^{1/3}$, the intermicellar interaction is modeled via a screened Coulomb potential and $S(Q)$ under mean spherical approximation. In this analysis, the only unknown parameter in interparticle structure factor, $S(Q)$ is the effective monomer charge, α.

The data in Figure 4 corresponding to different surfactants 1 and 2a−2e were first analyzed in terms of eq 2. N, ν, a, and α were taken as the parameters for the fit. The solid lines in Figure 4 are the calculated curves. The semimajor axis a ($3N\nu/4\pi b^2$) was obtained from knowledge of the above parameters. The values of N, α, a, and b are given in Table 2. The effects of concentration and temperature on size parameters for 2b ($m = 4$) were also obtained by similar methods.

■ RESULT AND DISCUSSION

Synthesis. To develop cleavable surfactants, an amide linkage in the surfactant molecule has been introduced (Figure 1). In order to synthesize the amide-containing surfactants (Supporting Information), first an intermediate activated amide, N-dodecyl-1-bromoethanamide was synthesized by reacting dodecylamine with bromoacetyl bromide. N-dodecyl-1-bromoethanamide was then reacted with trimethylamine to synthesize the monomeric surfactant dodecyl N-ethanamide N,N,N-trimethylammonium bromide (1) quantitatively. For synthesizing amide-bearing cationic gemini surfactants, another set of intermediates N,N,N′,N′-tetramethyl-α,ω-diaminoalkanes was prepared by reacting α,ω-dibromoalkanes with dimethylamine with almost quantitative yield (98−100%). N,N,N′,N′-tetramethyl-α,ω-diaminoalkanes were then reacted with N-dodecyl-1-bromoethanamide to synthesize the gemini surfactants 2a−2e. The surfactants were characterized by FT-IR, ¹HNMR, and mass spectrometry.

Critical Micelle Concentration. The electrical conductivity of surfactant solution is known to change at different rates below and above the CMC. Surfactant molecules dissociate completely at low concentrations, and their specific conductivities increase linearly with the increase in concentration. Although the concentration increases even after the CMC, the rate of increase in conductivity is less as compared to that of below CMC as some of the counterions are bound to the

Table 3. Effect of Spacer Length (m) in Micellar Systems of Amide Bearing Cationic Surfactants on Q Value[a]

micellar system	aggregation no., N	fractional charge, α	semimajor axis, a (Å)	semiminor axis, $b = c$ (Å)	a/b
2a ($m = 2$)	245	0.12	199.6	19.0	10.50
2b ($m = 4$)	123	0.19	105.0	19.0	5.52
2c ($m = 6$)	60	0.26	54.3	18.9	2.87
2d ($m = 8$)	45	0.34	44.7	18.4	2.43
2e ($m = 12$)	47	0.27	57.3	17.2	3.33

[a]All of the SANS spectra were recorded at 30 °C using 25 mM surfactant concentration.

micelle causing a reduction of the effective charge of the micelle. Hence, the plot of the conductivity vs concentration below and above the CMC produces two straight lines which intersect at the CMC (Figure 2). The CMC for each surfactant was therefore determined by plotting the specific conductivities (κ) of surfactant solutions as a function of concentrations (C). For aqueous solution of each surfactant, reproducible breaks were observed in κ vs C plots indicating the onset of aggregation.

The CMC values of gemini surfactants were found to be very low (CMC = 0.08−0.19 mM) and are 23−55 times lesser than corresponding monomeric analogue (CMC = 4.4 mM). This is due to the presence of two hydrophilic head groups and two hydrophobic tails connected by a hydrophobic methylene spacer in the gemini surfactants as compared to only one hydrophilic headgroup and one hydrophobic tail in the monomeric surfactant which causes the former to have higher aggregation tendency in water. The CMC values of gemini surfactants were found to decrease from 0.19 mM (for $m = 2$) to 0.08 (for $m = 12$) with the increase in spacer length (Figure 3). This is likely due to the enhancement in the hydrophobicity with increase in spacer length, which facilitates the molecule to aggregate in water. Nevertheless, it must be noted that there is not much variation of the CMC of the gemini surfactants with the spacer length. This fact is important in the uses and applications of gemini surfactants because it indicates that the properties (chemical, physical and biological) of a gemini surfactant can be much modified by acting on the nature and length of the spacer, without affecting the CMC substantially. The CMC value obtained using the same method for DTAB (16.1 mM) has been found to be in good agreement with the CMC value reported for DTAB in the literature.[56] However, the CMC value (4.4 mM) of the monomeric surfactant **1** was found to be very low as compared to DTAB. This could be attributed to the fact that the presence of an amide moiety in surfactant **1** probably facilitates enhanced aggregation through intermolecular hydrogen bonding along with the hydrophobic interaction thus leading to a lower CMC for surfactant **1**.

A quantitative measurement of the degree of ionization (α), a fraction of an ionic surfactant's counterions dissociated from the micelles, leaving the micelles charged, is crucial to understand many aspects of the micellar aggregates. For example, the stability,[57] morphological switchover such as spherical to ellipsoidal,[58] the viscoelastic behavior,[59] etc. were had been found to depend on α. The rate of a chemical reaction between organic substrate and hydrophilic ions that can "bind" to the micelles was also found to depend on the value of α.[57,58] For practical purposes, the degree of ionization is very important in various applications that demand the micelle as a charged interface such as gene delivery.[59] So, we measured the degree of ionization (α) of the newly synthesized micelles. It was calculated from the ratio of the slopes of the two straight lines above and below the CMC (Table 1). It was found that

the degree of ionization is higher for the gemini surfactants (0.28−0.43) as compared to the monomeric surfactant (0.26). This is probably due to the presence of two cationic headgroups and two bromide counterions in the gemini surfactants as compared to only one cationic headgroup and one counterion in monomeric surfactant. Furthermore, it was also observed that the degree of ionization increases with the increase in spacer chain length (from 0.28 for $m = 2$ to 0.43 for $m = 12$) (Figure 3). It is known that the degree of ionization depends on the size of micelles where larger micelles has greater tendency to attract counterions than a smaller micelle.[60] As it is evident from the subsequent section of our SANS study (Table 2 and 3) that the size of the micelles decreases with the increase in spacer length, consequently the α value increases upon increase in spacer length.

Small Angle Neutron Scattering (SANS) Studies. In a neutron scattering experiment, a beam of neutron is directed toward the sample under examination and the intensities of the neutron scattering in various directions are measured. Since neutrons are scattered by the nuclei of atoms in the sample, even isotopes of the same elements differ in their scattering power. Thus, by taking micellar aggregates in D_2O rather than in H_2O, the scattering densities of various regions can be obtained, as deuterons and protons differ widely in their respective scattering capacities. From the earlier reports, SANS measurements have been found to provide useful information regarding the shapes of various self-organizing systems in a noninvasive manner.[37−48] Consequently, we examined how these amide bearing cleavable gemini surfactant micelles adopt different morphologies and internal packing arrangements in aqueous media depending on their spacer chain length (m) using the SANS experiments.

First, we report the results of the measurements of neutron cross sections from the micellar solutions of the gemini surfactants **2a−2e** along with monomeric surfactant **1** in D_2O at 50 mM at 30 °C. Measurements have covered Q ranges from 0.017 to 0.352 Å^{-1} and the data is shown in Figure 4. SANS distributions for **1** ($m = 0$) and **2a−2e** ($m = 2, 4, 6, 8,$ and 12) showed well-defined peaks (Figure 4). The reason behind the origin of this peak is because of a corresponding peak in the interparticle structure factor $S(Q)$. Usually, this peak occurs at $Q_m \approx 2\pi/d$, where d is the average distance between the micelles. As the Q_m was found to vary with spacer length (m) for gemini surfactants, it can be concluded that the number density (n) of micelles was not the same in above samples even when they have identical concentration (50 mM). The above observations further indicate that the aggregation number of the micelle, N, depends on the spacer chain length m. However, it was not apparent that the micelles were spherical. In the following analysis, we, therefore, assumed them to be prolate ellipsoids ($a \neq b = c$), sphere being a special case of that.

For all of the gemini surfactants, **2a−2e** in D_2O at 50 mM, the aggregation number, N, appeared to decrease from 585 to

65 with the increase in spacer chain length from $m = 2$ to 8 and again increase to 104 for $m = 12$ (Table 2). On the contrary, the effective fractional charge (α) on micelles increased from 0.09 to 0.23 with increasing spacer chain length from **2a** ($m = 2$) to **2d** ($m = 8$) and again decreased to 0.19 with further increase in the spacer length (for $m = 12$). Since spheroids and ellipsoids differ in terms of curvature, larger effective charge would be expected for a spheroidal micelle and smaller effective charge would be associated for an ellipsoidal structure. Thus, it appears that for gemini micelles with m value 8, the shape of the micelles progressively becomes less elliptical (i.e., more spherical) at 50 mM concentration. On the other hand, higher aggregation number, N and substantially lower values of fractional charge, α for micelles with $m = 2$ and 4 indicate more ellipsoidal morphology. This is further supported by the changes in a/b values as a function of spacer chain length. Within the gemini surfactants, a/b values decreased from 19.63 to 3.33 as m values increased from $m = 2$ to 8 and then again increased to 5.72 for $m = 12$. These findings are in good agreement with the earlier reports of SANS study of dimeric surfactants.[47,48]

The aggregation number (N) and the fractional charge (α) of micellar solution of the monomeric surfactant **1** ($m = 0$) at identical conditions (at 30 °C and 50 mM) was found to be 96 and 0.23, respectively. The ratio of semimajor and semiminor axes (a/b value) was 1.83 for the monomeric surfactant **1**. It is evident form Table 2 that a/b value of the surfactant **1** is much lower than that of gemini surfactants thus indicating that the micellar aggregates from the monomeric surfactant is more spheroidal compared to gemini surfactants under the experimental conditions.

It is interesting to note that compared to DTAB, the monomeric surfactant **1** ($m = 0$) micelles have a considerably higher aggregation number (for DTAB, $N = 70$ whereas for surfactant **1**, $N = 107$) at same concentration and temperature (at 100 mM and 30 °C). Furthermore, a/b value of the surfactant **1** is almost double than that of DTAB (a/b value for surfactant **1** is 2.14 whereas a/b value for DTAB is 1.22). Consequently, these results indicate that the micellar growth of the surfactant **1** is much more pronounced compared to the micellar growth of DTAB in aqueous solution at identical conditions. Although DTAB also possesses only one Me$_3$N$^+$ headgroup and a single hydrocarbon chain, in a micellar aggregate the surfactant **1** is expected to be more "tightly" associated because of the presence of an amide unit [−NH−C(O)−] that links the Me$_3$N$^+$ headgroup with the hydrocarbon chain. The presence of an amide linkage probably facilitates intermolecular association among surfactants through hydrogen bonding interactions in organized assemblies. Also, as these amide linkages are located near the Stern-layer region of the micelles, hydrogen-bonding interactions among the surfactant molecules may also operate via interfacially adhering with water molecules.

In order to have further insight about the role of amide group on the aggregation behavior of the gemini surfactants containing amide group, the aggregation number (N) and a/b values of the micellar aggregate formed by the surfactant **2c** ($m = 6$) were compared with that of the conventional gemini surfactants having same spacer length (12−6−12 and 16−6−16). The N value of 12−6−12 (CMC = 1.01 mM) was found to be 36[8] at 100 mM and 30 °C, while the N value for the surfactant **2c** ($m = 6$) was ~4 times higher ($N = 125$) even at 50 mM and 30 °C. This suggests that amide group enhances

the aggregation of these surfactants in aqueous solution possibly through hydrogen bonding even more strongly as compared to the corresponding monomeric surfactant. The aggregation behavior of **2c** was even superior to the surfactant 16−6−16 (CMC = 0.043 mM, $N = 97$).[48] The effect of the amide group is further evident from the respective a/b values of the surfactants (2.21 for 12−6−12; 3.08 for 16−6−16; and 5.19 for **2c**).

In order to find the effect of the spacer chain length on the aggregation properties of the gemini surfactants at lower concentration, SANS experiments were also performed at 25 mM for all the gemini surfactants ($m = 2$ to $m = 12$) at 30 °C. Results of the measurements of neutron cross section from the micellar solution of gemini surfactants as a function of m values at lower concentration (25 mM) showed the similar behavior as that of at 50 mM at 30 °C (Figure 5). The peak at the SANS
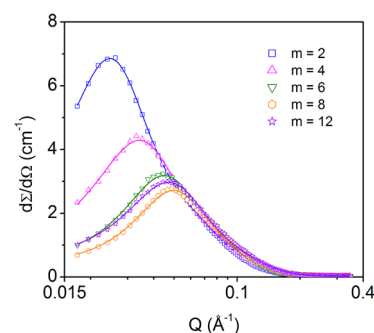
Figure 5. SANS distributions of the aqueous solution of gemini surfactants **2a**−**2e** ($m = 2$−12) at 25 mM at 30 °C. The lines shown are theoretical fits and the solid marks are experimentally determined data points.

distribution curve was shifted at higher Q values as the spacer length increases (Figure 5). It was also observed that the distribution curves broaden with the spacer as found previously for the higher concentration (50 mM). However, at 30 °C, it was observed that a/b values were much higher for all the gemini surfactants especially with spacer $m = 2$ and 4 at higher concentration (50 mM) compared to that of at 25 mM thus indicating the greater tendency of aggregation and as well as more ellipsoidal morphology (Table 2 and 3) of the gemini surfactants at higher concentration.

The aggregation number (N) of the gemini surfactants was found to vary from 245 to 45 with spacer chain length with the lowest N value observed for $m = 8$ at 25 mM and at 30 °C. In general, it was found that the aggregation numbers are much lower for the gemini surfactants at lower concentration (245−45 at 25 mM to 585−65 at 50 mM) which indicates strong dependence of aggregation tendency of the gemini surfactants on the spacer length at different concentrations (Table 2 and 3). Furthermore, the higher a/b values for the gemini surfactants particularly with shorter spacer length ($m \leq 4$) at higher concentration than that of at 25 mM indicate the microstructures formed by the gemini surfactants are more ellipsoidal (Table 2 and 3).

The effect of the spacer chain length on the micellar properties of the amide bearing gemini surfactants was also investigated at higher temperature (60 °C) for all the gemini surfactants at 50 mM. The distribution of scattering cross section was shown in Figure 6. It was found that the aggregation number, N for all the gemini micellar systems is
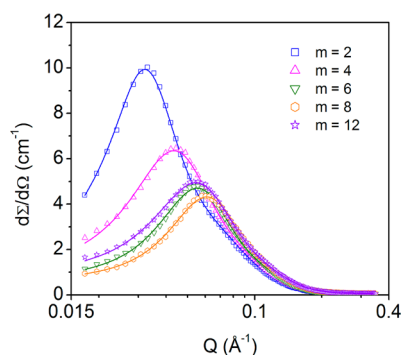
Figure 6. SANS distributions of the aqueous solution of gemini surfactants **2a**−**2e** (m = 2−12) at 50 mM at 60 °C. The lines shown are theoretical fits and the solid marks are experimentally determined data points.

Figure 7. SANS distributions from **2b** gemini (m = 4) micelles at different concentrations (12.5- 50 mM) at 30 °C. The lines shown are theoretical fits and the solid marks are experimentally determined data points.

much lower at 60 °C than that of at 30 °C at identical concentration (50 mM). This observation implies that higher temperature suppresses the tendency of micellar growth (Table 4). The aggregation number, N of the gemini surfactants (m = 2−12) was found to be 276−42. Thus the decrease in aggregation numbers is much greater for the gemini surfactants **2a**−**2e** at higher temperature (276−43 at 60 °C to 585−65 at 30 °C) indicating that the temperature has pronounced effect on the micellar aggregation of the gemini surfactants (Table 2 and 3). This is further evident from the a/b values as given in Table 2 and 3. However, in order to have better understanding of the effect of variation of temperature and concentration on the micellar aggregation of the gemini surfactants, we have performed the SANS experiments at different concentrations and temperatures for the gemini surfactant **2b** (m = 4).

Effect of Surfactant Concentration. The effect of variation of concentration on SANS distributions at 30 °C was studied with **2b** (m = 4) surfactant system and are shown in Figure 7. As previously mentioned, the peak in $d\Sigma/d\Omega$ arises from intermicellar interference effects and occurs at $Q_m = 2\pi/d$, where d is average distance between the micellar particles. With an increase in concentration, the interparticle distance decreases and hence the peak shifts to higher Q values. The concentration variation range examined was from 12.5 to 50 mM, and it is observed that the calculated distributions give the peak positions in $d\Sigma/d\Omega$ with a good concordance with experimentally determined points. Furthermore, it was found that the peak in the measured distribution broadens with significant shifts in the position with the decrease in the surfactant concentration.

As can be seen from Figure 7, the peak position shifts toward higher Q region which implies that the interparticle distance (as $Q_m = 2\pi/d$) decreases. These results indicate an increase in the number-density of **2b** surfactant micelles at higher concentration and are in agreement with the previous findings.[48] This
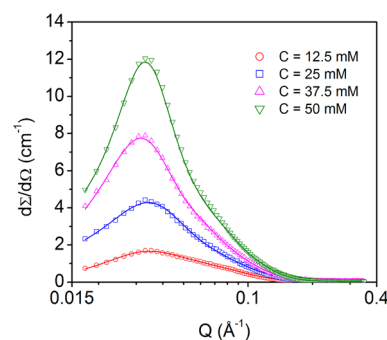
explains why the aggregation number N increased appreciably (from 62 to 320) with the increase in concentration from 12.5 to 50 mM. With the increase in surfactant concentration, the axial ratio (a/b) was found to increase from 2.62 to 12.88 (Table 5). This in turn indicates that micellar shape tends to become more oblate ellipsoidal (thread like micellar shape) as the concentration of the surfactant increases. Since the shape of the surfactant microstructure varies with respect to concentration, the interactions among charged headgroups of the gemini **2b** units and water in the Stern layer region of the micelle seem to play an important role in determining the micellar shape. The effective fractional charge (α) on the gemini units of **2b** changes from 0.21 to 0.14 as the concentration increases from 12.5 to 50 mM. The decrease in α with the increase in concentration further proves that the micellar system progressively becomes more elliptical.

Effect of Temperature. The effect of temperature variation on the microstructure of the gemini surfactants had been studied earlier.[48,61] In order to find out the effect of the temperature on the micellar aggregates, we also performed SANS experiments at various temperatures. Figure 8 shows the variation of neutron cross sections for **2b** (m = 4) micellar system with the increase in temperature. The neutron cross sections were found to shift at higher Q values and the peak in the measured distribution broadens as the temperature is increased (from 30 to 60 °C).

The aggregation number N for **2b** (m = 4) at 50 mM, decreased from 320 to 109 and the fractional charge was found to increase from 0.14 to 0.19, with increase in temperature (Table 6). With the increase in temperature, the degree of ionization and hence the magnitude of electrostatic repulsion among the positively charged surfactant molecules increases leading to reduction in the aggregation number. Since ellipsoidal morphology relates to a smaller effective charge, increasing temperature appears to induce toward less ellipsoidal
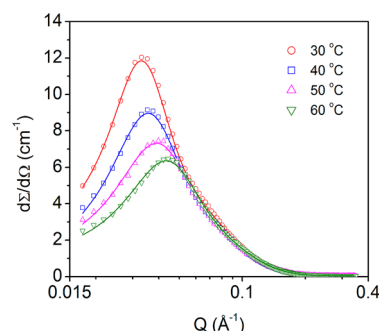
Table 4. Effect of Spacer Length (m) in Micellar Systems of Amide Bearing Cationic Surfactants on Q Value[a]

micellar system	aggregation no., N	fractional charge, α	semimajor axis, a (Å)	semiminor axis, b = c (Å)	a/b
2a (m = 2)	276	0.13	249.1	19.5	12.77
2b (m = 4)	109	0.18	88.0	19.5	4.51
2c (m = 6)	56	0.29	53.1	18.4	2.89
2d (m = 8)	43	0.37	45.1	17.8	2.53
2e (m = 12)	52	0.26	62.0	17.4	3.56

[a]All of the SANS spectra were recorded at 60 °C using 50 mM surfactant concentration.

Table 5. Effect of Concentration in Micellar Systems of Amide Bearing Cationic Surfactants 2b ($m = 4$) on Q Value at 30°C

concentration, C (mM)	aggregation no., N	fractional charge, α	semimajor axis, a (Å)	semiminor axis, $b = c$ (Å)	a/b
12.5	62	0.21	50.8	19.4	2.62
25	123	0.19	105.0	19.0	5.53
37.5	247	0.17	199.8	19.5	10.25
50	320	0.14	253.8	19.7	12.88

Figure 8. SANS distributions from 50 mM **2b** gemini ($m = 4$) micelles at various temperatures (30−60 °C). The lines shown are theoretical fits and the solid marks are experimentally determined data points.

Table 6. Effect of Temperature in Micellar Systems of Amide Bearing Cationic Surfactants 2b ($m = 4$) on Q Value at 50 mM Concentration

T (°C)	aggregation no., N	fractional charge, α	semimajor axis, a (Å)	semiminor axis, $b = c$ (Å)	a/b
30	320	0.14	253.8	19.7	12.88
40	221	0.16	170.1	20.0	8.51
50	154	0.17	117.8	20.1	5.86
60	109	0.19	88.0	19.5	4.51

structures (more spheroidal) for **2b**. This observation is also supported by the gradual decrease in a/b values from 12.88 to 4.51 with increase in temperature.

CONCLUSION

Micelle formation by the cleavable amide bearing gemini surfactants with the varying spacer chain length ($m = 2, 4, 6, 8,$ and 12) were investigated and compared with the corresponding monomeric surfactant by conductivity and SANS studies. The CMC values of gemini surfactants were found to be 23−55 times lesser than corresponding monomeric analogue (CMC = 4.4 mM). With the increase in the spacer chain length CMC was found to decrease whereas degree of ionization was found to increase. From the detailed measurements of SANS cross sections, it was also found that the extent of growth and variation of shapes of the micellar aggregates of these gemini micelles depend strongly on the spacer chain length and are more pronounced with short spacer length ($m \leq 4$). It was observed that with an increase in concentration, the aggregation number (N) and size of the micelles increased. On the contrary, with the increase in temperature, the aggregation number (N) decreased and the shape of the micellar aggregates were found to be less ellipsoidal (more toward spheroidal morphology).

ASSOCIATED CONTENT

S **Supporting Information**

Synthesis, FT-IR, ^{1}H NMR, and HRMS spectral data of *N*-dodecyl-1-bromoethanamide, dodecyl *N*-ethanamide *N,N,N*-trimethylammonium bromide (**1**), *N,N,N′,N′*-tetramethyl-α,ω-

diaminoalkanes, and dimeric amphiphiles (**2a−2e**). This material is available free of charge via the Internet at http://pubs.acs.org.

AUTHOR INFORMATION

Corresponding Author

*Telephone: +91-80-2208-2565. Fax: +91-80-2208-2627. E-mail: jayanta@jncasr.ac.in.

Notes

The authors declare no competing financial interest.

REFERENCES

(1) Menger, F. M. *Angew. Chem., Int. Ed. Engl.* **1991**, *30*, 1086−1099.
(2) Zana, R.; Talmon, Y. *Nature* **1993**, *362*, 228−230.
(3) Borse, M. S.; Devi, S. *Adv. Colloid Interface* **2006**, *123−126*, 387−399.
(4) Deng, M.; Li, J.; Liu, J.; Ma, X.; Wang, Y. *Colloid Surf., A* **2010**, *356*, 97−103.
(5) Zana, R. *J. Colloid Interface Sci.* **2002**, *248*, 203−220.
(6) Rodríguez, A.; Graciani, M. M.; Cordobés, F.; Moya, M. L. *J. Phys. Chem. B* **2009**, *113*, 7767−7779.
(7) You, Y.; Zhao, J.; Jiang, R.; Cao, J. *Colloid Polym. Sci.* **2009**, *287*, 839−846.
(8) Chavda, S.; Kuperkar, K.; Bahadur, P. *J. Chem. Eng. Data* **2011**, *56*, 2647−2654.
(9) Menger, F. M.; Littau, C. A. *J. Am. Chem. Soc.* **1991**, *113*, 1451−1452.
(10) Karaborni, S.; Esselink, K.; Hilbers, P. A. J.; Smit, B.; Karthauser, J.; van Os, N. M.; Zana, R. *Science* **1994**, *266*, 254.
(11) Oda, R.; Huc, I.; Homo, J. C.; Heinrich, B.; Schmutz, M.; Candau, S. *Langmuir* **1999**, *15*, 2384−2390.
(12) Kabir-ud-Din; Fatma, W; Khan, Z. A.; Dar, A. A. *J. Phys. Chem. B* **2007**, *111*, 8860−8867.
(13) Oda, R.; Huc, I.; Schmutz, M.; Candau, S. J.; MacKintosh, F. C. *Nature* **1999**, *399*, 566−569.
(14) Lu, T.; Huang, J.; Liang, D. *Langmuir* **2008**, *24*, 1740−1744.
(15) Macián, M.; Seguer, J.; Infante, M. R.; Selve, C.; Vinardell, M. P. *Toxicology* **1996**, *106*, 1−9.
(16) Zana, R.; Xia, J. Gemini Surfactants: Synthesis. *Interfacial and Solution-Phase Behavior, and Applications*; Marcel Dekker, Inc.: New York, 2004.
(17) Borde, C.; Nardello, V.; Wattebled, L.; Laschewsky, A.; Aubry, J. M. *J. Phys. Org. Chem.* **2008**, *21*, 652−658.
(18) Páhi, A. B.; Király, Z.; Mastalir, A.; Dudás, J.; Puskás, S.; Vágó., A. *J. Phys. Chem. B* **2008**, *112*, 15320−15326.
(19) Kirby, A. J.; Camilleri, P.; Engberts, J. B. F. N.; Feiters, M. C.; Nolte, R. J. M.; Söderman, O.; Bergsma, M.; Bell, P. C.; Fielden, M. L.; Rodríguez, C. R. G.; Guédat, P.; Kremer, K.; McGregor, C.; Perrin, C.; Ronsin, G.; van Eijk, M. C. P. *Angew. Chem., Int. Ed.* **2003**, *42*, 1448−1457.

(20) Bajaj, A.; Paul, B.; Indi, S. S.; Kondaiah, P.; Bhattacharya, S. *Bioconjugate Chem.* **2007**, *18*, 2144−2158.

(21) Bombelli, C.; Caracciolo, G.; Profio, P. D.; Diociaiuti, M.; Luciani, P.; Mancini, G.; Mazzuca, C.; Marra, M.; Molinari, A.; Monti, D.; Toccacieli, L.; Venanzi, M. *J. Med. Chem.* **2005**, *48*, 4882−4891.

(22) Caillier, L.; Givenchy, E. T.; De.; Levy, R.; Vandenberghe, Y.; Geribaldi, S.; Guittard, F. *J. Colloid Interface Sci.* **2009**, *332*, 201−210.

(23) Kresge, C. T.; Leonowicz, M. E.; Roth, W. J.; Vartuli, J. C.; Beck, J. S. *Nature* **1992**, *359*, 710−712.

(24) Beck, J. S.; Vartuli, J. C.; Roth, W. J.; Leonowicz, M. E.; Kresge, C. T.; Schimitt, K. D.; Chu, C. T. W.; Olsan, D. H.; Sheppard, E. W. *J. Am. Chem. Soc.* **1992**, *114*, 10834−10834.

(25) Huo, Q.; Margolese, D. I.; Ciesla, U.; Feng, P.; Gier, T. E.; Sieger, P.; Leon, R.; Petroff, P. M.; Schüth, F.; Stucky, G. D. *Nature* **1994**, *368*, 317−321.

(26) Holmberg, K. *J. Colloid Interface Sci.* **2004**, *274*, 355−364.

(27) Bhattacharya, S.; Biswas, J. *Nanoscale* **2011**, *3*, 2924−2930.

(28) Olkowska, E.; Polkowska, Z.; Namiésnik, J. *Chem. Rev.* **2011**, *111*, 5667−5700.

(29) Funasaki, N.; Ohigashi, M.; Hada, S.; Neya, S. *Langmuir* **2000**, *16*, 383−388.

(30) Hoffmann, H.; Sturmer, A. *Tenside Surf. Deterg.* **1993**, *30*, 335−342.

(31) Schnur, J. M. *Science* **1993**, *262*, 1669−1676.

(32) Menger, F. M.; Keiper, J. S. *Angew. Chem., Int. Ed.* **2000**, *39*, 1906−1920.

(33) Tehrani-Bagha, A. T.; Holmberg, K. *Langmuir* **2010**, *26*, 9276−9282.

(34) Stjerndahl, M.; Holmberg, K. *J. Surf. Deterg.* **2005**, *8*, 331−337.

(35) Thorsteinsson, T.; Másson, M.; Kristinsson, K. G.; Hjálmarsdóttir, M. A.; Hilmarsson, H.; Loftsson, L. *J. Med. Chem.* **2003**, *46*, 4173−4181.

(36) Haldar, J.; Kondaiah, P.; Bhattacharya, S. *J. Med. Chem.* **2005**, *48*, 3823−3831.

(37) Reynolds, P. A.; Gilbert, E. P.; White, J. W. *J. Phys. Chem. B* **2001**, *105*, 6925−6932.

(38) Tanford, C. *J. Phys. Chem.* **1972**, *76*, 3020−3024.

(39) Berr, S. S. *J. Phys. Chem.* **1987**, *91*, 4760−4765.

(40) Berr, S. S.; Jones, R. R. M. *Langmuir* **1988**, *4*, 1247−1257.

(41) Berr, S. S.; Jones, R. R. M.; Johnson, J. S., Jr. *J. Phys. Chem.* **1992**, *96*, 5611−5614.

(42) Pilsl, H.; Hoffmann, H.; Hoffmann, S.; Kalus, J.; Kencono, A. W.; Lindner, P.; Ulbricht, W. *J. Phys. Chem.* **1993**, *97*, 2745−2754.

(43) Goyal, P. S.; Menon, S. V. G.; Dasannacharya, B. A.; Thiyagarajan, P. *Phys. Rev.* **1995**, *51E*, 2308−2315.

(44) Haldar, J.; Aswal, V. K.; Goyal, P. S.; Bhattacharya, S. *Angew. Chem., Int. Ed.* **2001**, *40*, 1228−1232.

(45) Haldar, J.; Aswal, V. K.; Goyal, P. S.; Bhattacharya, S. *J. Phys. Chem. B* **2001**, *105*, 12803−12808.

(46) Haldar, J.; Aswal, V. K.; Goyal, P. S.; Bhattacharya, S. *J. Phys. Chem. B* **2004**, *108*, 11406−11411.

(47) Hirata, H.; Hattori, N.; Ishida, M.; Okabayashi, H.; Frusaka, M.; Zana, R. *J. Phys. Chem.* **1995**, *99*, 17778−17784.

(48) De, S.; Aswal, V. K.; Goyal, P. S.; Bhattacharya, S. *J. Phys. Chem.* **1996**, *100*, 11664−11671.

(49) Hayter, J. B.; Penfold, J. *Colloid Polym. Sci.* **1983**, *261*, 1022−1030.

(50) Hayter, J. B.; Penfold, J. *Mol. Phys.* **1981**, *42*, 109−118.

(51) Hansen, J.-P.; Hayter, J. B. *Mol. Phys.* **1982**, *46*, 109−118.

(52) Hayter, J. B.; Penfold, J. *J. Chem. Soc., Faraday Trans. 1* **1981**, *77*, 1851−1863.

(53) Chen, S. H. *Annu. Rev. Phys. Chem.* **1986**, *37*, 351−399.

(54) Chen, S. H.; Lin, T. L. *Methods of Experimental Physics*; Academic Press: New York, 1987.

(55) Mortensen, K. *J. Phys.: Condens. Matter* **1996**, *8*, A103−A124.

(56) Ström, C.; Hansson, P.; Jönsson, B.; Söderman, O. *Langmuir* **2000**, *16*, 2469−2474.

(57) Soldi, V.; Keiper, J.; Romsted, L. S.; Cuccovia, I. M.; Chaimovich, H. *Langmuir* **2000**, *16*, 59−71.

(58) Oda, R.; Narayanan, J.; Hassan, P. A.; Manohar, C.; Salkar, R. A.; Kern, F.; Candau, S. J. *Langmuir* **1998**, *14*, 4364−4372.

(59) Wang, Y.; Dubin, P. L.; Zhang, H. *Langmuir* **2001**, *17*, 1670−1673.

(60) Tsao, H. K. *J. Phys. Chem. B* **1998**, *102*, 10243−10247.

(61) De, S.; Aswal, V. K.; Goyal, P. S.; Bhattacharya, S. *J. Phys. Chem. B* **1998**, *102*, 6152−6160.